

THE DUST, NEBULAR EMISSION AND DEPENDENCE ON QSO RADIO PROPERTIES OF THE ASSOCIATED MG II ABSORPTION LINE SYSTEMS

PUSHPA KHARE

CSIR Emeritus Scientist, IUCAA, Ganeshkhind, Pune, 411007, India

DANIEL VANDEN BERK

Physics Department, St. Vincent College, Latrobe, PA 15650, USA

HADI RAHMANI

School of Astronomy, Institute for Research in Fundamental Sciences (IPM), PO Box 19395-5531, Tehran, Iran

DONALD G. YORK

Department of Astronomy and Astrophysics, University of Chicago, Chicago, IL 60637; Enrico Fermi Institute, University of Chicago, Chicago, IL 60637

Draft version October 24, 2018

ABSTRACT

We studied dust reddening and [O II] emission in 1730 Mg II associated absorption systems (AAS; relative velocity with respect to QSOs, $\leq 3000 \text{ km s}^{-1}$; in units of velocity of light, β , ≤ 0.01) with $0.4 \leq z_{abs} \leq 2$ in the SDSS DR7, focusing on their dependence on the radio and other QSO properties. We used control samples, several with matching radio properties to show (i) AAS in radio detected (RD) QSOs cause 2.6 ± 0.2 times higher dust extinction than those in radio undetected (RUD) ones which, in turn, cause 2.9 ± 0.7 times the dust extinction in the intervening systems; (ii) AAS in core-dominated QSOs cause 2.0 ± 0.1 times higher dust extinction than in lobe-dominated QSOs; (iii) occurrence of AAS is 2.1 ± 0.2 times more likely in RD QSOs than in RUD QSOs and 1.8 ± 0.1 time more likely in QSOs having black holes with masses larger than $1.23 \times 10^9 M_{\odot}$ than in those with lower mass black holes; (iv) there is excess flux in [O II] $\lambda 3727$ emission in the composite spectra of the AAS samples compared to those of the control samples, which is at the emission redshift. Presence of AAS enhances the O II emission from the AGN and/or the host galaxy. This excess is similar for both RD and RUD samples, and is 2.5 ± 0.4 times higher in lobe-dominated compared to core-dominated samples. The excess depends on the black hole mass and Eddington ratio. All these point to the intrinsic nature of the AAS except for the systems with $z_{abs} > z_{em}$ which could be infalling galaxies.

Subject headings: Quasars: absorption lines — ISM: abundances, dust, extinction — Galaxies: high-redshift

1. INTRODUCTION

The origin of associated absorption systems (AAS) in the spectra of QSOs with $\beta < 0.01^1$ (the relative velocity of the AAS with respect to the QSO, hereafter V , $< 3000 \text{ km s}^{-1}$) is not very well understood. Possibilities for their origin include (i) interstellar/halo clouds in the host galaxy (e.g. Chelouche et al. 2008), (ii) material in the core of the active galactic nucleus (AGN), within 10 pc of the black hole (Barlow & Sargent 1997), (iii) material within 30 kpc of the AGN, accelerated by starburst shocks from the inner galaxy (e.g. Fu & Stockton 2007) and (iv) clouds in galaxies clustered around the QSO (e.g. Wild et al. 2008). The study of properties of a large sample of such systems and in particular, their correlation with radio and other properties of the parent QSO, should provide clues towards discerning between various scenarios.

Several studies of the dependence of the properties of the AAS on QSO radio properties have been undertaken in the past. Some studies found the frequency of occurrence of AAS to depend on the radio properties of the QSO (e.g. Anderson et al. 1987; Foltz et al. 1988; Ganguly et al. 2001; Baker et al. 2002) Other studies failed to find such de-

pendence (e.g. Vestergaard 2003) but concluded that differences in the results could probably be attributed to various differences in selection of the relatively small samples (50-100 systems). An excess of AAS in radio loud QSOs was also found by Wild et al. (2008) in a large sample of SDSS QSOs.

In a previous study (Vanden Berk et al. 2008, hereafter V08), based on Sloan Digital Sky Survey (SDSS) data release 3 (DR3), we had studied the average dust extinction and average abundances of a homogeneous sample of 407 AAS (with $\beta < 0.01$; $V < 3000 \text{ km s}^{-1}$) using the method of composite spectra (York et al. 2006; hereafter Y06). Definite evidence of dust in the AAS was obtained by comparing the composite spectra of the absorber sample with that of a non-absorber (control) sample matching in z_{em} and i magnitude on a one to one basis. The dust was found to be of SMC type with no evidence for the presence of a 2175 \AA absorption feature. The amount of dust extinction and the frequency of occurrence of AAS in the sample were found to depend on radio properties of the QSOs.

A much larger (by a factor of > 4) sample of Mg II systems is now available from the SDSS DR7 (Shen & Menard 2012; hereafter SM12). With this increase in size, it should be possible to gain further understanding of the associated absorbers. In particular, we can study the dependence of their dust ex-

¹ β is the relative velocity of the absorption systems with respect to the systemic redshift of the QSO in units of velocity of light

tion and star formation rate (SFR) (as measured from the [O II] λ 3727 emission line flux), on radio and other properties e.g. the black hole mass (M_{BH} , determined from the widths of various emission lines) and Eddington ratio (R_{Edd} which is the ratio of bolometric luminosity of the object to its Eddington luminosity) of the QSOs. Black hole mass may be indicative of its age.

In a merger-driven model of AGNs, supermassive black holes evolve through major mergers which give rise to starbursts and also to accretion onto the nuclear black hole (Sanders et al. 1988; Hopkins et al. 2005, 2006). In such models large amounts of gas and dust are funneled inward which fuels the black hole and also causes the obscuration of the young QSO. The dust might be cleared during a transitional phase resulting in the emergence of a luminous blue QSO. In this picture, reddening is correlated with the evolutionary stage of the QSO. Recently, Shen & Menard (2012) have shown that QSOs with associated absorbers with $\beta < 0.005$ ($V < 1500 \text{ km s}^{-1}$), exhibit enhanced star formation. They suggest that these absorbers could be large-scale outflows indicative of the transitional phase in a merger-driven evolutionary scenario for QSOs. Based on the smaller dust extinction and SFR, they conclude that the systems with $\beta > 0.005$ ($V > 1500 \text{ km s}^{-1}$) originate in intervening absorbers.

In this paper we present the results of our study of the SM12 sample of AAS, using the method of composite spectra. We particularly focus on the dependence of AAS properties on the radio and other properties of the QSOs. The details of the sample and sub-samples thereof as well as the method of analysis are presented in section 2, results are presented in section 3 and conclusions are presented in section 4.

2. SAMPLE SELECTION AND ANALYSIS

2.1. Main sample and sub-samples

As mentioned above we used the sample compiled by SM12 (their Table 1) from the SDSS DR7. Their sample contains 1937 systems in non-BAL QSOs with $\beta < 0.01$ ($V < 3000 \text{ km s}^{-1}$), spanning the redshift range of 0.4-2 and with rest equivalent width $W_{\text{Mg II}}$ ranging from 0.22 to 6.8 \AA . Five of these have $W_{\text{Mg II}} < 0.3 \text{\AA}$. There are 92 sight-lines having two AAS each and six sight-lines having three AAS each. For this study, we focused primarily on QSOs having only one AAS along their lines of sight, although some statistics for QSOs with multiple AAS are also presented. Also, we restricted our sample to $W_{\text{Mg II}} > 0.3 \text{\AA}$ so that our results can be compared with those of V08 and Y06. Our full sample, S1, thus consists of 1730 AAS having $W_{\text{Mg II}} \geq 0.3 \text{\AA}$.

We compiled several sub-samples from S1 by dividing it roughly in half, based on various QSO and absorber properties: $W_{\text{Mg II}}$, i magnitude, radio properties, M_{BH} , and R_{Edd} . Among the radio properties, we consider whether the QSOs have been radio detected (RD) or undetected (RUD) in the FIRST survey, as well as whether the sources are core dominated (CD) or lobe dominated (LD). Among our sample of 1730 AAS, 263 have been detected while 1341 have been undetected in the FIRST survey. 67 of the 263 RD QSOs, 67 are lobe dominated while 196 are core dominated. The division of S1 based on β was done using the criterion of SM12 ($\beta < 0$ ($V < 0 \text{ km s}^{-1}$), $0 \leq \beta < 0.005$ ($0 \leq V < 1500 \text{ km s}^{-1}$) and $\beta \geq 0.005$ ($V \geq 1500 \text{ km s}^{-1}$) so that our results can be compared with their conclusions. The radio and other properties (e.g. M_{BH} and R_{Edd}) of QSOs used for defining the sub-samples were taken from Shen et al. (2011).

Throughout this study, we use the emission redshifts as given by Hewett & Wild (2010) and use the relative velocities of AAS with respect to these as given by SM12. Details of the sub-samples are given in Table 1 which lists number of systems and the average values of $W_{\text{Mg II}}$, z_{abs} , β , i magnitude, M_{BH} (this is given in units of M_{\odot} throughout the paper), and R_{Edd} .

2.2. Composite spectrum

The method of forming composite spectra is described in detail by Y06 and V08. We describe it briefly here. First, the spectra of individual QSOs, corrected for Galactic reddening, were shifted to the absorber/QSO rest-frame and resampled onto a common pixel-to-wavelength scale. Pixels flagged by the spectroscopic pipeline as possibly bad in some way (Stoughton et al. 2002) were masked and not used in constructing the composites. Also masked were the pixels within 5 \AA of the expected line positions of detected intervening absorption systems unrelated to the target system. The geometric mean of all contributing spectra was then calculated for each pixel. The median/mean composite for [O II] emission line studies was obtained by first fitting the continuum to $\sim 30 \text{\AA}$ wide regions around 3727 \AA in the QSO/absorber rest-frame and then resampling the continuum subtracted spectra to a common wavelength scale.

We calculate the $E(B - V)$ values for various samples by comparing the composite spectrum of each sample with that of the corresponding control samples (sample of QSOs not having AAS, matching one to one in z_{em} and i magnitude with the QSOs in the absorber sample), and fitting an SMC curve (Pei 1992) to the extinction curve so obtained. In deriving this extinction curve, we have normalized the two composites at 3000 \AA , which was the value used by SM12. However, we have verified that normalizing at longer wavelengths does not affect the $E(B - V)$ values. The values are also independent of whether QSO rest-frame or absorber rest-frame composites are used. To construct the absorber rest-frame composite of the control sample, the spectrum of each QSO in the sample was shifted to the rest-frame of the absorber towards the corresponding QSO (matching in i magnitude and z_{em}) in the absorber sample. The typical 1σ errors in the derived $E(B - V)$ values are generally smaller than 0.003 (The errors of the relative flux density values are calculated using the variance formula for the propagation of errors of a geometric mean. see Y06 and V08 for a detailed analysis of errors). The Milky Way extinction curve does not fit well for any of the samples, and the dust seems to be of SMC type, with no evidence of the 2175 \AA bump. The $E(B - V)$ values so determined are given in the third column of Table 2. We note that any difference in the $E(B - V)$ values of different sub-samples indicates (i) a difference in the dust column density caused either by different gas column density or by different dust-to-gas ratio, or (ii) different properties of the dust. In QSO absorbers, the extinction curve is found to be same (SMC type) for all the samples. Thus, the dust properties appear to be similar. The dust content is known to be correlated with $W_{\text{Mg II}}$ (Y06, V08, Wild et al. 2006, Menard et al. 2011). Thus, the dust column may be correlated with $W_{\text{Mg II}}$ and in case we find the values of $E(B - V)$ to be different for sub-samples having similar $W_{\text{Mg II}}$, then it may indicate a difference in the dust-to-gas ratio for the two sub-samples.

2.3. Control samples

For sub-samples S1-S8 and S13-S16, we used the control samples which were used by SM12 (and kindly provided by them). In the construction of these samples the radio properties of the QSOs were not taken into account which is also the case for these sub-samples. However, it is known that the RD QSOs are intrinsically redder than the RUD QSOs (e.g. see Figure 6 of Kimball et al. 2011; hereafter K11) irrespective of presence/absence of AAS. The geometric mean composites for the samples of 4714 RD and 65253 RUD DR7 QSOs in K11 were kindly provided to us by the authors. Fitting an SMC extinction curve to the ratio of the two composites, we estimate the relative $E(B - V)$ between the two samples to be 0.042. Another selection effect could be important: the SDSS QSO target selection is made on the basis of (blue) color. However a number of QSOs which may not satisfy the color selection criteria are also observed based on other criteria, mainly, their luminosity in other bands like the radio and hence need not have typical QSO colors and could be reddened by selection. About 70 QSOs in both S9 and S10 are not color selected, i.e. a much higher fraction of QSOs in the RD sample are not color selected and hence could be reddened. In addition, the intrinsic reddening in RD QSOs could also depend on their radio morphology. On the basis of a complete sample of 4714 SDSS QSOs in DR7 with determined radio properties and with FIRST flux $S20 > 2$ mJy, K11 found that radio sources with unresolved cores have higher reddening. It is therefore necessary to construct control samples also based on their radio properties for sub-samples S9-S12.

We constructed such control samples for sub-samples S9 and S10 (matching one to one in z_{em} and i magnitude) from the RD and RUD QSOs (respectively) in SDSS DR7 which do not have AAS in their spectra. The $E(B - V)$ values obtained using these control samples should be independent of any intrinsic reddening in the QSOs caused by their radio properties and should reflect the reddening caused by the presence of AAS. As the control sample now has the matching radio properties, non-color selection should be equally probable in the sub-sample and its control sample. We also constructed control samples of lobe dominated and core dominated QSOs from such QSOs in DR7 without AAS for S11 and S12 respectively. The values of $E(B - V)$ for all these sub-samples (S9-S12), given in Table 2 are calculated using these control samples with matching radio properties in addition to matching z_{em} and i magnitude.

3. RESULTS

3.1. Dependence of the frequency of occurrence of AAS on the radio and other properties of QSOs

Among DR7 non-BAL QSOs with redshifts between 0.4 and 2.0, 68755 QSOs have been observed by the FIRST radio survey (Becker, White, and Helfand 1995). Out of these, 6366 are radio detected, 4668 are core-dominated, and 1698 are lobe-dominated. Thus, the fraction of RD QSOs among all QSOs in DR7 in the relevant redshift range is 0.093 ± 0.001 . Out of 1730 QSOs in our sample (having a single AAS each), 1604 have been observed by FIRST: 263 are RD, 196 are core-dominated, and 67 are lobe-dominated. Additionally, out of the 98 QSOs in the SM12 sample having multiple AAS, 90 have been observed by FIRST: 30 are RD (26 being CD) while 60 are RUD QSOs. The fraction of RD QSOs among the QSOs having AAS (single or multiple) is 0.17 ± 0.01 . The occurrence of AAS is higher by a factor of 2.1 ± 0.1 in RD QSOs compared to RUD QSOs. Similarly, while a fraction

$\sim 0.11 \pm 0.02$ of RD QSOs in our sample have multiple AAS, the fraction is $\sim 0.045 \pm 0.006$ for RUD QSOs in this sample: the incidence of multiple AAS is $\sim 2.5 \pm 0.6$ times as likely in RD QSOs compared to the RUD ones. These values remain unchanged (to within 1σ) if the sample is restricted to the systems with $\beta < 0.005$ ($V < 1500$ km s $^{-1}$, which are intrinsic systems according to the results of SM12. Thus, the dependence of incidence of AAS on radio properties is the same for all systems with $\beta < 0.01$. The occurrence of AAS is significantly related to the radio properties of the QSOs which is consistent with the results of most previous studies mentioned in section 1.

The fraction of core-dominated QSOs among the RD DR7 QSOs is $\sim 0.73 \pm 0.01$ while in our sample, selected by the presence of (single or multiple) AAS, it is $\sim 0.76 \pm 0.07$. The presence of AAS seems to be independent of the morphology of the radio source. We caution that the numbers here are small and the statistics may not be very meaningful. These results are unchanged if we restrict the analysis to systems with $\beta < 0.005$.

Among the 73181 non-BAL QSOs in the redshift range of 0.4 and 2.0 in DR7, 47521 QSOs have $\log(M_{BH}) \leq 9.1$ while 25660 have $\log(M_{BH}) > 9.1$. AAS are present in a fraction of 0.028 ± 0.001 of QSOs having smaller black hole mass while for more massive black holes the values are 0.033 ± 0.001 . The values are thus significantly different. The corresponding values for QSOs with $\log(R_{Edd}) \leq -0.81$ and > -0.81 are 0.024 ± 0.001 and 0.022 ± 0.001 respectively. Thus, considering the black hole mass, QSOs with older black holes have a higher frequency of occurrence of AAS. No such difference exists for samples of lower and higher Eddington ratios.

3.2. Reddening

The reddening for S1 can be directly compared with the reddening obtained for intervening systems by Y06 as both samples are from the SDSS data and use the same method of composite spectra and as the selection criterion for the two samples are identical except for the range of relative velocities with respect to the QSOs. The $E(B - V)$ for S1 is 3.2 ± 0.8 times higher than for the intervening systems for which the $E(B - V)$ is 0.013. A comparison with the results of V08 shows that the $E(B - V)$ values obtained here are larger by factors between 1.5-2, while the dependence of $E(B - V)$ on $W_{Mg II}$, i magnitude and radio properties is same. This could partly be because of the higher fraction (15.2%) of RD QSOs in our sample as compared to (9.9%) in the sample of V08 and partly a small sample effect.

As seen from Table 2, the reddening is higher in fainter QSOs (S3) compared to brighter ones (S2). This could be due to the higher average $W_{Mg II}$ (1.61 \AA) in S3 compared to that (1.32 \AA) in S2 as reddening is sensitive to the $W_{Mg II}$ values (see $E(B - V)$ values for S4 and S5 in Table 2). Reddening in AAS with $\beta > 0.005$ (S8) is significantly smaller than the values for samples with smaller β (S6 and S7) as found by SM12, but is still significantly higher by a factor of 2.1 ± 0.5 than that in intervening systems. The sub-sample with higher M_{BH} (S14) is brighter (see Table 1) than that with lower M_{BH} (S13), while the $E(B - V)$ values are equal for both sub-samples. The sub-sample with lower R_{Edd} (S15) is more reddened compared with the sub-sample having higher Eddington ratio (S16).

3.2.1. Dependence of reddening on radio properties of the QSOs

It is clear from the $E(B - V)$ values that the AAS in RD QSOs are indeed dustier (by a factor of 2.6 ± 0.2) than those in RUD QSOs. Among the average properties (See Table 1) of RD and RUD QSOs (sub-samples S9 and S10), the RD QSOs have only marginally higher $W_{\text{Mg II}}$, i band brightness, and R_{Edd} . The excess extinction in the RD sub-sample over that in the RUD QSOs thus, can not be possibly be accounted for by the differences in these average properties. As the difference in reddening in RD QSOs can not be accounted by the difference in $W_{\text{Mg II}}$ therefore, as noted in section 2.2, the AAS towards RD QSOs may have higher dust-to-gas ratio. Differences can also be seen among the core and lobe-dominated sub-samples, in that core-dominated QSOs are 2.0 ± 0.1 times more reddened. Both classes of RD QSOs (S11 and S12) are significantly more reddened compared to the RUD QSOs. This is consistent with the results of V08 but is in contrast to the results of K11 who found that only radio sources with unresolved cores have higher reddening, and other classes of RD QSOs have reddening comparable to that of the RUD QSOs. Also, the reddening in AAS in RUD QSOs is 2.9 ± 0.7 times higher than that in the intervening systems (Y06).

To check if the reddening in RD QSOs with AAS is correlated with $W_{\text{Mg II}}$, we divided sub-sample S9 into two roughly equal halves (S9a and S9b) depending on $W_{\text{Mg II}}$. The results for these are given in Tables 2. These confirm that the RD QSOs with stronger Mg II absorption lines are considerably more reddened compared to those having weaker Mg II lines; the difference between the $E(B - V)$ values of the two samples being 0.093. The average $W_{\text{Mg II}}$ for the two sub-samples S9a and S9b are 2.5 and 0.9 Å, which are very similar to those of sub-samples S5 and S4 (2.1 and 0.83 Å) respectively, for which the $E(B - V)$ differ by only 0.029. Thus RD QSOs have a stronger dependence of reddening on $W_{\text{Mg II}}$. We also divided the RUD sub-sample (S10) into two halves (S10a and S10b) depending on $W_{\text{Mg II}}$. The results for these are given in the last rows of Tables 2. The average $W_{\text{Mg II}}$ values for sub-samples S10a and S10b and the difference in the $E(B - V)$ values for these samples are similar to that between the values for sub-samples S5 and S4.

The main conclusion from this study is that the AAS in RD QSOs are significantly more reddened than those in RUD QSOs which, in turn, are significantly more reddened than the intervening systems.

3.3. Emission lines from host galaxies/absorbers

3.3.1. Excess emission flux in QSOs with AAS

SM12 found excess emission flux in the [O II] $\lambda 3727$ line (hereafter EEFOII) in the composite spectrum of QSOs having AAS with $\beta < 0.005$ over that in the composite spectra of the control sample of QSOs without AAS both made at the emission rest frame. These results were interpreted as indicating that the EEFOII originates in the host galaxies of QSOs having AAS with $\beta < 0.005$, and that it is a measure of SFR in those galaxies. We discuss the [O II] emission further below.

In order to study the emission lines, we constructed continuum-subtracted composites (median and mean) of various sub-samples as well as those of the corresponding control samples in the QSO rest-frame. We also constructed corresponding composites in the absorber rest-frames. For this, the spectrum of each QSO in the control sample was shifted to the rest-frame of the absorber towards the corresponding QSO (matching in i magnitude and z_{em}) in the absorber sample.

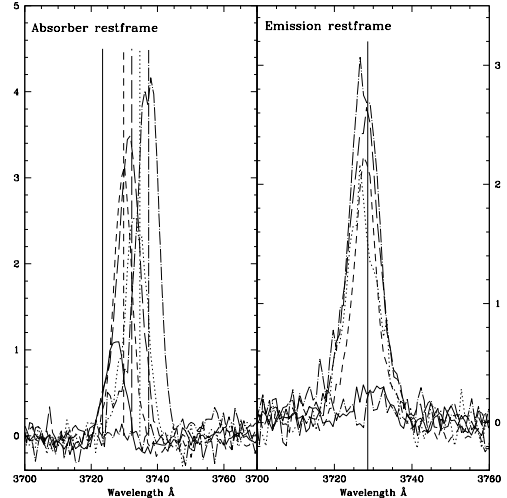


FIG. 1.— Left panel shows the absorber frame residual spectra (difference between the absorber rest-frame composites of the absorber sample and those of corresponding control sample) for various β dependent samples. The samples plotted are: S6 (solid line), $0 < v < 200 \text{ km s}^{-1}$ ($\beta = 0 - 0.0007$) (short dashed line), $200 \text{ km s}^{-1} < v < 400 \text{ km s}^{-1}$ ($\beta = 0.0007 - 0.0013$) (long dashed line), $400 \text{ km s}^{-1} < v < 600 \text{ km s}^{-1}$ ($\beta = 0.0013 - 0.002$) (dotted line) and $600 \text{ km s}^{-1} < v < 800 \text{ km s}^{-1}$ ($\beta = 0.002 - 0.0027$) (dash-dotted line). The vertical lines indicate the effective wavelengths of the [O II] doublet (3728.6 \AA which is the value used by Hewett & Wild) at the mean values of the relative velocities for each sample. The right panel shows the same but for emission rest-frame composites.

We observed that the median composite is not very meaningful when constructed in the absorber rest-frame as the peak of the [O II] $\lambda 3727$ emission line which gets contribution from the AGN and its host galaxy at the emission redshift) is shifted by different amounts (depending on the value of β) and as a result the total flux in the line in the median composite is not the same as that in the median composites in the emission rest-frame. This problem does not appear if we construct the mean composites (without clipping in the emission line region). We have therefore, used the mean composites for measuring the EEFOII. The values of the ratio of the [O II] flux in the composite spectrum of the sample to that in the composite of the corresponding control sample for various sub-samples using the control samples described in section 2 are listed in column 4 of Table 2. In most cases these are independent of whether the mean composites are made in the emission or absorption rest-frames, we mention the exception to this below.

It can be seen that a significant EEFOII is seen for all sub-samples. The magnitude of EEFOII depends on values of QSO brightness, β , black hole mass, Eddington ratio, and on radio morphology. The EEFOII does not depend on the strength of absorption lines (S4 and S5). This is different from what is seen for the intervening systems where the [O II] emission flux is proportional to $W_{\text{Mg II}}$ (Noterdaeme et al. 2010; Menard et al. 2011). As will be seen below, this is due to the different fractions of RD and RUD QSOs in these samples. The sub-samples with lower M_{BH} and higher R_{Edd} have lower EEFOII. Finally, the EEFOII in the S7 sample ($0 < \beta < 0.005$) is much higher than that in S6 ($\beta < 0$) and S8 ($\beta \geq 0.005$). It thus appears that the hosts of AAS with β between 0 and 0.005 are different from those with $\beta < 0$ and > 0.005 .

In order to confirm that the EEFOII arises in the emission rest-frame, we have plotted in the left panel of Figure

TABLE 1
DEFINITIONS AND PROPERTIES OF SUB-SAMPLES OF AAS.

Sample number	Selection criterion	No. of systems	$\langle W_{\text{Mg II}} \rangle$ in \AA	$\langle z_{em} \rangle$	$\langle \beta \rangle$ $\times 10^3$	$\langle m_i^a \rangle$	$\text{Log}(\langle M_{\text{BH}}^b \rangle)$	$\text{Log}(\langle R_{\text{Edd}} \rangle)$
S0	Sample of SM12	1937	1.43	1.27	1.3	18.56	9.04	-0.64
S1	Full sample	1730	1.46	1.28	2.16	18.59	9.04	-0.63
S2	$m_i \leq 18.68$	862	1.32	1.26	2.46	18.11	9.15	-0.58
S3	$m_i > 18.68$	868	1.61	1.30	1.85	19.08	8.93	-0.69
S4	$W_{\text{Mg II}} \leq 1.24 \text{\AA}$	866	0.83	1.26	2.27	18.46	9.06	-0.64
S5	$W_{\text{Mg II}} > 1.24 \text{\AA}$	864	2.10	1.30	2.04	18.73	9.01	-0.62
S6	$\beta < 0.0$	510	1.49	1.29	-1.39	18.62	9.05	-0.67
S7	$0.0 \leq \beta < 0.005$	841	1.47	1.22	1.83	18.64	9.04	-0.70
S8	$\beta \geq 0.005$	379	1.42	1.40	7.66	18.46	9.01	-0.47
S9	Radio-detected (RD)	263	1.67	1.18	1.79	18.45	9.03	-0.54
S10	Radio-undetected (RUD)	1341	1.43	1.30	2.25	18.62	9.04	-0.65
S11	Lobe-dominated (LD)	67	1.46	1.18	1.64	18.45	9.11	-0.42
S12	Core-dominated (CD)	196	1.74	1.18	1.85	18.45	9.01	-0.58
S13	$\text{Log}(M_{\text{BH}}) \leq 9.09$	874	1.47	1.12	2.23	18.72	8.66	-0.49
S14	$\text{Log}(M_{\text{BH}}) > 9.09$	856	1.46	1.44	2.08	18.47	9.42	-0.85
S15	$\text{Log}(R_{\text{Edd}}) \leq -0.81$	870	1.55	1.20	1.59	18.78	9.19	-1.09
S16	$\text{Log}(R_{\text{Edd}}) > -0.81$	860	1.38	1.36	2.73	18.41	8.88	-0.411

a: SDSS i magnitude, corrected for Galactic extinction.
b: In units of M_{\odot}

TABLE 2
 $E(B - V)$ AND [O II] $\lambda 3727$ FLUX EXCESS FOR SUB-SAMPLES OF AAS.

Sample number	Selection criterion	$E(B - V)^a$ w.r.t control samples	[O II] flux w.r.t control samples ^b
S1	Full sample	0.041	1.92 \pm 0.04
S2	$m_i \leq 18.68$	0.031	1.84 \pm 0.04
S3	$m_i > 18.68$	0.049	2.07 \pm 0.05
S4	$W_{\text{Mg II}} \leq 1.24 \text{\AA}$	0.026	1.9 \pm 0.05
S5	$W_{\text{Mg II}} > 1.24 \text{\AA}$	0.05-	1.94 \pm 0.04
S6	$\beta < 0.0$	0.047	1.32 \pm 0.05
S7	$0.0 \leq \beta < 0.005$	0.055	2.32 \pm 0.06
S8	$\beta \geq 0.005$	0.027	1.52 \pm 0.07
S9	Radio-detected (RD)	0.097	1.73 \pm 0.04
S10	Radio-undetected (RUD)	0.038	1.87 \pm 0.06
S11	Lobe-dominated (LD)	0.056	2.08 \pm 0.13
S12	Core-dominated (CD)	0.109	1.44 \pm 0.04
S13	$\text{Log}(M_{\text{BH}}) \leq 9.09$	0.038	1.76 \pm 0.04
S14	$\text{Log}(M_{\text{BH}}) > 9.09$	0.041	2.40 \pm 0.08
S15	$\text{Log}(R_{\text{Edd}}) \leq -0.81$	0.058	2.19 \pm 0.05
S16	$\text{Log}(R_{\text{Edd}}) > -0.81$	0.025	1.55 \pm 0.04
S9a ^c	RD, $W_{\text{Mg II}} > 1.4$	0.149	2.10 \pm 0.08
S9b ^d	RD, $W_{\text{Mg II}} \leq 1.4$	0.056	1.44 \pm 0.04
S10a ^e	RUD, $W_{\text{Mg II}} > 1.23$	0.057	2.38 \pm 0.13
S10b ^f	RUD, $W_{\text{Mg II}} \leq 1.23$	0.018	1.48 \pm 0.06

a: One σ errors in $E(B - V)$ are typically smaller than 0.003.
b: Ratio of flux in [O II] emission line in the sample composite to that in the composite of the corresponding control sample. Note that the control samples used for S9, S10, S11, S12 and for S9a, S9b, S10a and S10b have matching radio properties.
c: S9a: 129 systems belonging to sub-sample S9 and having $W_{\text{Mg II}} > 1.4 \text{\AA}$.
d: S9b: 134 systems belonging to sub-sample S9 and having $W_{\text{Mg II}} \leq 1.4 \text{\AA}$.
e: S10a: 666 systems belonging to sub-sample S10 and having $W_{\text{Mg II}} > 1.23 \text{\AA}$.
f: S10b: 675 systems belonging to sub-sample S10 and having $W_{\text{Mg II}} \leq 1.23 \text{\AA}$.

1, the excess flux in the [O II] line in the absorption rest-frame composite spectra of various β dependent sub-samples over that in the composite of the corresponding control samples. For this figure we constructed additional sub-samples having relative velocity between (i) 0 and 200 km s⁻¹ ($\beta = 0-0.0007$), (ii) 200 and 400 km s⁻¹ ($\beta = 0.0007-0.0013$), (iii) 400 and 600 km s⁻¹ ($\beta = 0.0013-0.002$), and (iv) 600 and 800 km s⁻¹ ($\beta = 0.002-0.0027$). The number of systems in these sub-samples are 214, 185, 110, and 106 respectively. It is clear that the line centers in the absorber rest-frame composites are progressively shifted towards longer wavelengths with increasing β values of the sub-samples. We have plotted the positions of the [O II] lines at the mean velocities of the samples as vertical lines. For all samples with $\beta > 0$, these are roughly consistent with the centers of the corresponding emission excess confirming that the [O II] emission is in the QSO rest-frame. For $\beta < 0$ sample the line shows up at $\sim 3728 \text{ \AA}$ in the absorber rest-frame composite. The [O II] emission for these systems occurs at the absorber rest-frame and does not show up in the emission rest-frame composite. It thus seems possible that these absorbers are galaxies which are falling towards the QSOs. In the right panel of Figure 1, we have plotted the difference between the composites of the same samples and the composites of the corresponding control samples in the emission rest-frame. The excess is centered around $\sim 3728 \text{ \AA}$ and clearly shows that the excess emission occurs at the QSO redshift as was observed by SM12, and may originate in the host galaxy of the individual QSOs. Note that the excess emission is not seen here for the $\beta < 0$ sample.

We have measured the FWHMs of the excess [O II] emission in the composites (like those plotted in the right panel of Figure 1) of various sub-samples and these values all fall between 8 and 10 \AA . To estimate the errors in FWHM caused by the errors in z_{em} , we generated 100 composite spectra for each of the samples plotted in Figure 1, each time choosing random z_{em} within the one sigma values given by given by Hewett & Wild (2010). These errors in z_{em} are smaller than 0.006 for QSOs in our sample and in most cases are in fact smaller than 0.0025. The one σ error in FWHMs as measured from the FWHMs of the of the 100 composites for each of the samples are all smaller than 0.5 \AA . The FWHMs, thus, are large and are very similar to the FWHMs of the [O II] emission lines themselves in the spectra of the composites of the control samples. It therefore appears that the excess flux originates in the same regions as the [O II] emission lines of QSOs.

3.3.2. Dependence of the EEFOII on radio properties

Figure 6 of K11 shows that the flux of the [O II] $\lambda 3727$ line is significantly higher in the geometric mean composite of all radio QSOs as compared to that for all RUD QSOs in DR7. K11 have also studied the dependence of emission line fluxes in the median composite spectra for several emission lines on the radio properties of the QSOs. They find that the fluxes depend on the type of radio sources (see their Figure 7).

In our samples the values of EEFOII in RD QSOs are similar to that in RUD QSOs (with AAS). The EEFOII for absorbers in the lobe-dominated QSOs (S11) however, is higher than that for the core-dominated QSOs (S12). Thus, on the whole the EEFOII in RD and RUD QSOs is same but in RD QSOs the EEFOII is dependent on the radio morphology. It is interesting to note that in CD QSOs it is even lower than that in the RUD QSOs.

A comparison of the EEFOII for the RD sub-samples S9a and S9b defined on the basis of $W_{Mg II}$, shows that among the RD QSOs, the EEFOII is much stronger in QSOs having AAS with larger $W_{Mg II}$. The same also holds if we divide the RUD sub-sample S10 into two halves (S10a and S10b) depending on $W_{Mg II}$. Thus, the EEFOII depends on the strength of the Mg II lines in the AAS in both RD and RUD sub-samples. This dependence on $W_{Mg II}$ is qualitatively similar to what has been found for intervening systems (Noterdaeme et al. 2010; Menard et al. 2011).

4. DISCUSSION

Using the largest sample of AAS compiled so far, we have found that the incidence of Mg II AAS significantly depends on the radio properties of the QSOs. Radio detected QSOs are 2.1 ± 0.2 times more likely to have AAS as compared to RUD QSOs. Among the RD QSOs, the incidence of AAS does not seem to depend on the morphology of the radio source. This is inconsistent with earlier studies (mentioned in section 1) that found that the incidence of AAS is either independent of the radio properties of the QSOs (Vestergaard 2003) or it is higher in lobe-dominated QSOs (e.g. Aldcroft et al. 1994). We also find a significantly higher frequency of occurrence of AAS in QSOs with higher black hole masses compared with that in QSOs with smaller black hole masses.

It is clear from our results that the radio properties of the QSOs play an important role in influencing the reddening properties of the AAS. The dust extinction is higher in the AAS in RD QSOs than that in RUD QSOs by a factor of 2.6 ± 0.2 . Among the RD QSOs, the CD QSOs are more reddened by a factor of 2.0 ± 0.1 as compared to the LD QSOs. The reddening in the AAS in RUD QSOs is also higher than that in the intervening systems (by a factor of 2.9 ± 0.7). For both types of QSOs (RD and RUD), the reddening in the AAS depends on the strength of absorption lines; AAS with stronger lines show higher reddening. Based on the dust extinction alone, the AAS in both RD and RUD QSOs appear to be intrinsic to the QSO. The reddening is insensitive to the black hole mass but depends on the Eddington ratio in the sense that AAS in QSOs having lower Eddington ratios have higher dust extinction.

The dust extinction is found to be similar in AAS with $\beta < 0$ and with β between 0 and 0.005. The AAS with $\beta > 0.005$ are found to have smaller dust extinction by a factor of 1.7-2.0, however, the extinction is higher than that in the intervening systems (Y06) by a factor of 2.1 ± 0.5 , and therefore those AAS may not be intervening as suggested by SM12.

We note that there is always a selection effect acting against the very dusty systems which will not be observable in a flux limited survey. This however, applies both to the AAS as well as the intervening systems. Thus, the difference in the dust content of these two types of systems as obtained by comparing our results with those of Y06 is real as both are samples are taken from the SDSS. We have earlier shown (Khare et al. 2007), from a study of abundances in samples of DLAs and sub-DLAs observed at high resolution and also the average abundances in SDSS Mg II systems at redshifts similar to what we are studying here, that the obscuration bias is not likely to be important. Either very dusty systems do not exist or there may be a bi-modal distribution of dust and there may exist a population of completely dust obscured QSOs. Our results do not apply to such a population.

We have clearly demonstrated that the excess emission in the [O II] line originates at the emission redshift of the QSOs

(except for the $\beta < 0$ sample for which it occurs close to absorption redshift). This could be due to star formation in the host galaxy. However, for all sub-samples, the FWHM of the excess flux distribution is large ($\sim 8-10 \text{ \AA}$) and is similar to the FWHM of the total [O II] emission. Thus, the EEFOII may also originate in the same regions in the parent AGN and the host galaxy which emit the [O II] line and the presence of AAS enhances the O II emission from these regions.

In the the whole sample, the EEFOII does not depend on the Mg II equivalent width because of the different fractions of RD and RUD QSOs in the $W_{\text{Mg II}}$ dependent sub-samples. This is clear from the fact that when we consider the RD and RUD samples separately, the EEFOII is significantly higher for QSOs having AAS with larger $W_{\text{Mg II}}$, similar to what is observed for the intervening absorbers. The values of the EEFOII are within the range of fluxes determined for intervening Mg II systems (Noterdaeme et al. 2010). The EEFOII is similar for the RD and RUD QSOs; however, among the RD QSOs, the EEFOII is higher for the LD QSOs as compared to the CD QSOs. Thus, the dust extinction and EEFOII seem to be anti-correlated among the CD and LD QSOs, which is expected except that the dust extinction seems to be too small to explain the difference in EEFOIIs. The EEFOII does depend on the M_{BH} and R_{Edd} . EEFOII is higher in AAS in QSOs having higher M_{BH} and having lower R_{Edd} .

5. CONCLUSIONS

We have studied the properties of associated absorption systems in the redshift range of 0.4 to 2.0, in the spectra of 1730 SDSS QSOs. The main conclusions are as follows:

1. The average dust extinction is found to be of SMC type with no evidence for the 2175 \AA bump.
2. The dust extinction is 3.2 ± 0.8 times greater than in the intervening Mg II absorbers with similar selection criteria.
3. By using the control samples comprised only of RD, RUD, lobe-dominated and core-dominated QSOs, we find that (a) the AAS in RD QSOs are 2.6 ± 0.2 times more dusty compared to the AAS in RUD QSOs; (b) the reddening due to AAS in RD QSOs has a stronger dependence on $W_{\text{Mg II}}$ compared to that in RUD QSOs; (c) among the RD QSOs, the AAS in the core-dominated QSOs have 2.0 ± 0.1 times higher dust extinction compared to those in the lobe-dominated QSOs; (d) the reddening in the AAS in RUD QSOs is 2.9 ± 0.7 times higher than that in intervening absorbers.
4. The reddening does not depend on the black hole mass and thus its age.
5. The reddening does depend on the Eddington ratio, systems with smaller R_{Edd} have higher reddening.
6. The occurrence of AAS is 2.1 ± 0.5 times more likely in RD QSOs compared to RUD QSOs.
7. The occurrence of multiple AAS is 2.5 ± 0.6 times more likely in RD QSOs than in RUD QSOs.
8. Among the RD QSOs, the frequency of occurrence of AAS appears to be independent of the radio morphology.

9. The frequency of occurrence of AAS depends on black hole mass, QSOs with larger M_{BH} have higher rate of incidences. Thus, the incidence rate is higher for older black holes.
10. The EEFOII in the AAS samples over that in the control samples originates at the QSO redshift, and is consistent with its origin in the QSO. The width of the excess emission is large (FWHM $\sim 8-10 \text{ \AA}$) and is similar to the width of the [O II] line itself. This indicates its origin in the [O II] emitting regions in the AGN and its host galaxy. The presence of AAS enhances the O II emission from the AGN and/or the host galaxy.
11. The EEFOII is similar for RD and RUD QSOs.
12. For the RD as well as for RUD QSOs, the EEFOII depends on $W_{\text{Mg II}}$, such that the sub-sample with higher $W_{\text{Mg II}}$ has higher EEFOII in both cases.
13. Among the RD QSOs, the EEFOII is higher for the LD QSOs by a factor of 2.5 ± 0.4 compared to the CD QSOs.
14. The EEFOII depends on the mass of the black hole and the Eddington ratio such that QSOs with higher M_{BH} and lower R_{Edd} have higher EEFOII.
15. The EEFOII and dust extinction in CD and LD QSOs are anticorrelated.
16. The EEFOII is similar in magnitude to that found in the intervening absorbers.

Based on these results the AAS seem to have very different amount of dust and dust-to-gas-ratio as compared to the intervening systems, which seem to depend on the radio properties of the QSOs and also on the masses of the central black hole. The excess [O II] emission occurs at the QSO redshift. The width of the excess emission is similar to that of the emission lines in control samples. The AAS could therefore be intrinsic to the QSOs. Even with this large sample of AAS, we are possibly able to argue against only two of the possibilities, (i) and (iv), mentioned in section 1 for the origin of these systems. Their higher dust content compared to the intervening systems (even for $\beta > 0.005$ systems among the AAS) and its dependence on QSO properties argues against their origin in the ISM of galaxies clustering around the QSO, or in the ISM of the host galaxies themselves. One can argue that the jets from the AGN can influence the ISM in the host as well as the surrounding galaxies. However, the higher extinction is seen in both radio loud and radio quiet QSOs. Further studies are needed to distinguish between the other two scenarios.

ACKNOWLEDGMENTS

PK thanks CSIR, India for the grant of Emeritus Scientist fellowship. We would like to thank Shen and Menard for making the absorber sample as well as the control sample available. We are grateful to the referee for giving detailed comments and suggestions which helped improve the presentation in a significant way.

REFERENCES

- Aldcroft, T. L., Bechtold, J. & Elvis, M. 1994, *ApJS*, 93, 1
- Anderson, S. F., Weymann, R. J., Foltz, C. B. & Chaffee, F. H. 1987, *AJ*, 94, 278
- Baker, J. C., Hunstead, R. W., Athreya, R. M., Barthel, P. D., de Silva, E., Lehnert, M. D., & Suaners, R. D. E. 2002, *ApJ*, 568, 592
- Becker, R. H., White, R. L., & Helfand, D. J. 1995, *ApJ*, 450, 559
- Barlow, T. A., & Sargent, W. L. W. 1997, *AJ*, 113, 136
- Chelouche, D., Menard, B., Bowen, D. V., & Gnat, O. 2008, *ApJ*, 683, 55
- Foltz, C. B., Chaffee, F. H. Jr., Weyman, R. J., Anderson, S. F. 1988. In *QSO Absorption lines: Probing the Universe: Proceedings of the QSO Absorption line meeting*, Baltimore, MD, May 19-21, 1987. Cambridge and New York, Cambridge University Press, pp53-65
- Fu, H., & Stockton, A. 2007, *ApJ*, 666, 794
- Ganguly, R., Bond, N. A., Charlton, J. C., Eracleous, M., Brandt, W. N. & Churchill, C. W. 2001, *ApJ*, 549, 133
- Hewett, P. C. & Wild, V. 2010, *MNRAS*, 405, 2302
- Hopkins, P. F., Hernquist, L., Cox, T. J., et al. 2005, *ApJ*, 630, 705
- Hopkins, P. F., Hernquist, L., Cox, T. J., et al. 2006, *ApJS*, 163, 1
- Khare, P., Kulkarni, V. P., Peroux, C. et al. 2007, *A&A*, 464, 487
- Kimball, A. E., Ivezić, Z., Witta, P. J. & Schneider, D. P. 2011, *AJ*, 141, 182 (K11)
- Menard, B., Wild, V., Nestor, D., Quidder, A., Zibetti, S., Rao, S. & Turnshek, D. 2011, *MNRAS*, 417, 801
- Noterdaeme, P. Srianand, R. & Mohan, V. 2010, *MNRAS*, 403, 906
- Pei Y. C., 1992, *ApJ*, 395, 130
- Sanders, D. B., Soifer, B. T., Elias, J. H., et al. 1988, *ApJ*, 325, 74
- Shen, Y., Richards, G. T., Strauss, M. A., et al. 2011, *ApJS*, 194, 45
- Shen, Y. & Menard, B. 2012, *ApJ*, 748, 131 (SM12)
- Stoughton C., Lupton, R. H.; Bernardi, M. et al., 2002, *AJ*, 123, 485.
- Vanden Berk, D. E., Khare, P., York, D. G, et al. 2008, *ApJ*, 679, 239 (V08)
- Vestergaard, M. 2003, *ApJ*, 599, 116
- Wild, V., Hewett, P. C. & Pettini, M. 2006, *MNRAS*, 367, 211
- Wild, V., Kauffmann, G., White, S., et al. 2008, *MNRAS*, 388, 227
- York, D. G., Khare, P., Vanden Berk, D. E., et al. 2006, *MNRAS*, 367, 945 (Y06)